SIRPα+ dendritic cells promote the development of fibroblastic reticular cells in murine peripheral lymph nodes

Komori, Satomi ; Saito, Yasuyuki ; Respatika, Datu ; Nishimura, Taichi ; Kotani, Takenori ; Murata, Yoji ; Matozaki, Takashi

(Citation)
European Journal of Immunology,49(9):1364-1371

(Issue Date)
2019-09

(Resource Type)
journal article

(Version)
Accepted Manuscript

SIRPα^{+} dendritic cells promote the development of fibroblastic reticular cells in murine peripheral lymph nodes

[1]Satomi Komori, [1]Yasuyuki Saito*, [1,2]Datu Respatika, [1]Taichi Nishimura, [1]Takenori Kotani, [1]Yoji Murata and [1]Takashi Matozaki*

[1]Division of Molecular and Cellular Signaling, Department of Biochemistry and Molecular Biology, Kobe University Graduate School of Medicine, Kobe 650-0017, Japan

[2] Division of Reconstruction, Oculoplasty, and Oncology, Department of Ophthalmology, Faculty of Medicine, Public Health, and Nursing, Gadjah Mada University, Yogyakarta 55281, Indonesia.

*Correspondence: Takashi Matozaki or Yasuyuki Saito, Division of Molecular and Cellular Signaling, Department of Biochemistry and Molecular Biology, Kobe University Graduate School of Medicine, 7-5-1 Kusunoki-cho, Chuo-ku, Kobe 650-0017, Japan. Tel.: +81-78-382-5600. Fax: +81-78-382-5619.

Email: matozaki@med.kobe-u.ac.jp or ysaito@med.kobe-u.ac.jp

Keywords: lymph node・stromal cell・fibroblastic reticular cell・dendritic cell・SIRPα

A list of abbreviations used:

SIRPα, signal regulatory protein α; DCs, dendritic cells; cDCs, conventional DCs; Pdpn, podoplanin; FRCs, fibroblastic reticular cells; LNs, lymph nodes; pLNs, peripheral LNs; CCL, CC-chemokine ligand; LECs, lymphatic endothelial cells; BECs, blood endothelial cells; TNF-α, tumor necrosis factor α; rTNF-α, recombinant TNF-α; TNFR, TNF receptor; LNSCs, lymph node stromal cells;

NF-κB, nuclear factor-κB; mAb, monoclonal antibody; BMDCs, bone marrow-derived DCs; LPS, lipopolysaccharide

Abstract

Nonhematopoietic stromal cells contribute to the organization and homeostasis of secondary lymphoid organs by producing cytokines and chemokines. The development and maintenance of these stromal cells are thought to be regulated by innate immune cells. Indeed, we recently showed that signal regulatory protein α (SIRPα)–positive dendritic cells (DCs) are essential for the proliferation and survival of podoplanin (Pdpn)–positive fibroblastic reticular cells (FRCs) in mouse spleen. We have now established an *in vitro* culture system for stromal cells (LNSCs) isolated from mouse peripheral lymph nodes. Activated DCs and tumor necrosis factor–α each promoted the proliferation of cultured LNSCs, most of which were found to be Pdpn$^+$ FRCs. Furthermore, ablation of SIRPα in CD11c$^+$ cells attenuated this effect of DCs on LNSC proliferation. Transplantation of activated DCs together with cultured LNSCs into the renal subcapsular space markedly increased the number of ER-TR7$^+$ stromal cells as well as induced the accumulation of T cells and increased the expression of *Ccl19* in the transplants. Ablation of SIRPα in CD11c$^+$ cells greatly impaired the development of LN-like structure in the transplants. Our findings thus suggest that SIRPα$^+$ DCs are important for the proliferation and differentiation of Pdpn$^+$ FRCs in peripheral LNs.

Introduction

In secondary lymphoid organs, antigen-presenting cells interact with naïve T cells and B cells to promote effective immune responses as well as to maintain peripheral tolerance [1]. These immune cells gather within a network of lymphoid organ stromal cells that comprise a variety of reticular cell and endothelial cell subsets [1-3]. In particular, podoplanin (Pdpn)–positive fibroblastic reticular cells (FRCs) organize the paracortex of lymph nodes (LNs) and the periarteriolar lymphoid sheath of the white pulp of the spleen [4]. FRCs generate a reticular network of collagen-rich fibrils that facilitates the interaction of T cells with dendritic cells (DCs) [5]. FRCs also produce CC-chemokine ligand (CCL) 19 and CCL21 as well as express adhesion molecules, all of which preferentially attract T cells and DCs [6]. In addition, endothelial cell subsets such as lymphatic endothelial cells (LECs) and blood endothelial cells (BECs) contribute to antigen distribution and lymphocyte migration in secondary lymphoid organs [7,8].

The development and maintenance of lymphoid organ stromal cells are regulated by innate lymphoid cells. Lymphoid tissue inducer (LTi) cells interact with mesenchymal precursors and thereby promote their differentiation into stromal organizer cells (or lymphoid tissue organizer cells), which in turn are thought to give rise to various stromal cell types through further interaction with hematopoietic cells [9]. This process depends on the interaction of lymphotoxin $\alpha_1\beta_2$, a membrane-anchored heterotrimeric protein expressed on the surface of LTi cells, with the lymphotoxin-β receptor (LTβR) of mesenchymal precursors [10]. LTi cells are also thought to be important for the formation of tertiary lymphoid tissue during inflammatory responses [11]. In addition, DCs play a key role in the development and homeostasis of lymphoid organ stromal cells, particularly FRCs. Activated DCs up-regulate expression of the Pdpn ligand C-type lectin–2, the engagement of which with Pdpn on FRCs results in FRC stretching and the rapid expansion of LNs [12,13]. DCs also express lymphotoxin $\alpha_1\beta_2$ and promote the survival of FRCs through its interaction with LTβR on FRCs [14].

We have recently shown that $CD4^+$ conventional DCs (cDCs) regulate the steady-state homeostasis of FRCs in the adult mouse spleen via the production of tumor necrosis factor receptor (TNFR) ligands such as tumor necrosis factor–α (TNF-α) [15].

Signal regulatory protein α (SIRPα) is a transmembrane protein of the immunoglobulin superfamily that is highly expressed in $CD4^+$ cDCs as well as in macrophages [16,17]. It possesses three immunoglobulin-like domains in its extracellular region and an immunoreceptor tyrosine-based inhibition motif that binds the protein tyrosine phosphatases Shp1 and Shp2 in its intracellular region [18,19]. We have recently demonstrated that SIRPα expressed on cDCs is indispensable for the homeostatic regulation of splenic FRCs [15]. However, it has remained unclear whether $SIRP\alpha^+$ DCs participate in the development of FRCs in peripheral LNs (pLNs).

We have now developed an *in vitro* culture system for mouse LN stromal cells (LNSCs), the majority of which were found to be $Pdpn^+$ FRCs. With the use of this culture system and renal subcapsular transplantation, we further examined the role of $SIRP\alpha^+$ DCs in the proliferation and differentiation of LNSCs.

Results and discussion

Characterization of primary cultured LNSCs

We first established an *in vitro* culture system for LNSCs (**Fig. 1A**) [20]. Indeed, the yield of $CD45^-$ LNSCs at day 6 was ~15 times that at day 0 (**data not shown**). At day 0 and day 6, $CD45^-$ LNSCs were separated into four different subsets on the basis of the surface expression of Pdpn and CD31 (**Fig. 1B**). Among $CD45^-$ LNSCs at day 6, FRCs were predominantly developed (~70%)(**Fig. 1B and C**). By contrast, neither FDC-$M1^+$ follicular DCs nor MadCAM-1^+ marginal zone reticular cells were detected in the cultures (**data not shown**). The cultured LNSCs manifested a spindle-shaped morphology associated with the presence of pronounced F-actin stress fibers (**Fig. 1D**). They also expressed the intermediate-filament protein desmin (**Fig. 1D**) [21]. Both FRC

and LEC subsets expressed CD44 and MHC class I, but not MHC class II (**Fig. 1E**). These results thus indicated that $Pdpn^{+}CD31^{-}$ FRCs were preferentially expanded in primary cultures of LNSCs, consistent with previous results obtained with primary cultures of splenic stromal cells [15].

Either TNFR or LTβR signaling is thought to promote the proliferation and survival of stromal cells, with the former activating the canonical nuclear factor–κB (NF-κB) pathway and the latter the noncanonical NF-κB pathway [22,23]. We therefore examined whether TNFR or LTβR signaling stimulates the proliferation of cultured LNSCs. Recombinant TNF-α (rTNF-α) and a monoclonal antibody (mAb) to LTβR each significantly increased the proliferation of LNSCs, with the effect of rTNF-α being greater than that of the anti-LTβR mAb (**Fig. 1F**). The combination of rTNF-α and the anti-LTβR mAb promoted LNSC proliferation to an extent greater than that apparent with either agent alone (**Fig. 1F**). Lymphotoxin was previously shown to increase the expression of chemokine and adhesion molecule genes through the noncanonical NF-κB pathway [23,24]. The anti-LTβR mAb increased the amounts of mRNAs for VCAM–1 and ICAM-1 in cultured LNSCs, whereas it had no effect on the abundance of *Ccl19*, *Ccl21*, and *IL7* mRNA (**Fig. 1G**).

Importance of SIRPα on DCs for the proliferation of LNSCs

We recently showed that $SIRP\alpha^{+}$ cDCs promote the proliferation and survival of cultured $Pdpn^{+}$ splenic stromal cells [15]. Furthermore, ablation of SIRPα in $CD11c^{+}$ cells resulted in marked attenuation of their stimulatory effect on the proliferation of cultured $Pdpn^{+}$ stromal cells [15]. We here found that bone marrow–derived DCs (BMDCs) that had been treated with lipopolysaccharide (LPS) markedly promoted the proliferation of cocultured LNSCs (**Fig. 2A**). Furthermore, this effect was significantly attenuated in cocultures of LNSCs with BMDCs isolated from $CD11c^{+}$ cell–specific SIRPα-deficient ($Sirpa^{\Delta DC}$) mice compared with those derived from control mice

homozygous for the corresponding floxed *Sirpa* allele (*Sirpa*$^{f/f}$ mice) (**Fig. 2A**). The expression level of CD47, as well as CD80, CD86 and MHC molecules on activated BMDCs was similar between *Sirpa*$^{f/f}$ and *Sirpa*$^{\Delta DC}$ mice (**Supporting Information Fig. 1**). By contrast, the up-regulation of TNF-α, but not IL-6 and IL-10, by LPS was specifically inhibited in BMDCs derived from *Sirpa*$^{\Delta DC}$ mice compared with those derived from *Sirpa*$^{f/f}$ mice (**Fig. 2B**). These results suggest that SIRPα on DCs is important for the production of TNF-α upon stimulation with LPS.

DCs promote the development of LNSCs and recruitment of T cells in a renal subcapsular transplant

To examine further the role of DCs in the differentiation of Pdpn^{+} LNSCs in pLNs, we prepared a collagen sponge scaffold in which cultured LNSCs (at day 6) and LPS-activated BMDCs were embedded and transferred it to the renal subcapsular space of recipient mice (**Fig. 3A**). Three weeks after transplantation, immunohistofluorescence analysis showed that staining for ER-TR7, which identifies FRCs [25], was significantly greater in grafts containing LNSCs and LPS-activated BMDCs than in those containing LNSCs alone (**Fig. 3B**). Moreover, the accumulation of Thy1.2^{+} T cells around ER-TR7^{+} stromal cells was increased in grafts containing LNSCs plus BMDCs (**Fig. 3B**). Consistent with these results, the absolute numbers of both CD45^{+} hematopoietic cells and TCRβ^{+} T cells were significantly increased in grafts containing LNSCs plus BMDCs compared with those containing LNSCs alone (**Fig. 3C**), whereas the numbers of B cells, CD11c^{+} DCs, and SSC^{hi} granulocytes were similar between the two groups (**Fig. 3C** and **Supporting Information Fig. 2A**). These findings were also consistent with those of a previous study showing that activated BMDCs are indispensable for the development of LN-like structure in renal subcapsular transplants [26]. Moreover, the abundance of *Ccl19* mRNA, a marker for functionally differentiated FRCs, was significantly up-regulated in grafts containing LNSCs together with BMDCs

(**Fig. 3D**), suggesting that the up-regulation of *Ccl19* mRNA in grafts was attributable to the increased number, as well as to the differentiation, of ER-TR7$^+$ stromal cells. Together, our observations thus implicated DCs in control of the proliferation and differentiation of LNSCs as well as in the recruitment of T cells in the renal subcapsular transplant model.

The ER-TR7$^+$ area of LNSC grafts was significantly reduced in those containing BMDCs isolated from *Sirpa*$^{\Delta DC}$ mice compared with those containing *Sirpa*$^{f/f}$ BMDCs (**Fig. 3E**). In addition, the absolute number of CD45$^+$ cells, as well as those of T cells and granulocytes, were significantly reduced in grafts consisting of LNSCs and BMDCs from *Sirpa*$^{\Delta DC}$ mice compared with those of LNSCs and *Sirpa*$^{f/f}$ BMDCs (**Fig. 3F** and **Supporting Information Fig. 2B**).

Concluding remarks

We have here shown that activated BMDCs promote the differentiation of Pdpn$^+$ FRCs both *in vitro* cultures of LNSCs and in the renal subcapsular transplant model. We also showed that SIRPα deficiency in BMDCs markedly attenuated this effect as well as the LPS-induced up-regulation of *Tnf* expression in these cells, suggesting that SIRPα$^+$ BMDCs promote the proliferation and differentiation of LNSCs likely through their production of TNF-α (**Supporting Information Fig. 3**). By contrast, we previously found that the absolute number of T cells, as well as that of FRCs, in pLNs did not differ between *Sirpa*$^{\Delta DC}$ and *Sirpa*$^{f/f}$ mice, suggesting that SIRPα$^+$ DCs are dispensable for the homeostasis of FRCs in pLNs under the steady-state condition [15]. Given that the TNF-mediated activation of FRCs *in vitro* culture and renal subcapsular transplant models mimic the development or remodeling of pLNs, SIRPα$^+$ DCs are likely important for regeneration of FRCs in secondary lymphoid organs during immune responses or viral infection [20,27], as well as for TNF-mediated activation of FRCs and the attraction of myeloid cells by CCL2 in non-classical lymphoid organs after

Salmonella infection [28], rather than for their maintenance under the steady-state condition.

Materials and methods

Animals, antibodies, and reagents

C57BL/6 mice were obtained from Japan SLC. *Sirpa*$^{f/f}$ and CD11c-*Cre*;*Sirpa*$^{f/f}$ (*Sirpa*$^{\Delta DC}$) mice were generated previously [29]. All mice were inbred at the Institute of Experimental Animal Research of Kobe University Graduate School of Medicine under specific pathogen–free conditions. Sex- and age-matched mice were studied at 8 to 12 weeks of age. All animal experiments were approved by the Institutional Animal Care and Use Committee of Kobe University (permits P140508-R1, P140905, and P150204) and were performed according to Kobe University Animal Experimentation Regulations. **Supporting Information Table 1** provides a list of antibodies, reagents and resources.

Stromal cell isolation and culture

Isolation and culture of LNSCs from pLNs (axillary, brachial, and inguinal) were described previously [20]. In brief, LNs were digested for 40 min at 37°C in RPMI 1640 containing collagenase P (0.2 mg/mL), dispase (0.8 mg/mL), DNase I (1 mg/mL,), and 2% FBS, and undigested fibrous material was removed by filtration through a 70-μm nylon mesh. The cells were cultured at a density of 4×10^5 cells/cm^2 in culture flasks containing α–MEM supplemented with 10% FBS and 1% penicillin-streptomycin. Nonadherent cells were removed after 24 h, and the remaining attached cells were cultured in the same medium for an additional 5 days. The cells were then harvested and enriched for CD45$^-$ cells with the use of anti-mouse CD45 microbeads and an autoMACS Pro Separator to yield LNSCs. In some experiments, LNSCs were further cultured overnight before stimulation of TNFR or LTβR with rTNF-α (20 ng/mL) or an agonistic mAb to LTβR (5 μg/mL), respectively.

Flow cytometry

For flow cytometric analysis, cells were washed twice with PBS containing 2% FBS and 2 mM EDTA (FACS buffer). They were incubated first with a mAb to mouse CD16/32, and then with specific mAbs. The cells were analyzed with a FACSVerse and FlowJo v10 software. All flow cytometric procedures have been performed following the guidelines for the use of flow cytometry and cell sorting in immunological studies [30]

Immunofluorescence analysis

Cultured LNSCs were fixed with 4% paraformaldehyde, incubated for 1 h at room temperature in blocking solution (PBS containing 3% BSA and 0.25% Triton X-100), and then stained overnight at 4°C with rhodamine-phalloidin or primary antibodies diluted in blocking solution. The cells were then washed with PBS, stained for 1 h at room temperature with secondary antibodies and DAPI in blocking solution. For immunohistofluorescence analysis of kidney capsule grafts, tissues were embedded in Tissue-Tec O.C.T. compound and frozen in liquid nitrogen. Cryostat sections were prepared at a thickness of 5 μm, fixed with methanol, and exposed to 3% bovine serum albumin in PBS at room temperature before incubation with antibodies diluted in the blocking buffer. Images were captured with a BZ-X700 microscope and were processed with Adobe Photoshop software. The areas of positively stained regions in images were determined with the use of ImageJ software and averaged for at least five sections per graft.

Isolation of BMDCs

Bone marrow cells were isolated from mouse femur and tibia. Fibrous material was removed by filtration through a 70-μm nylon mesh, and erythrocytes in the filtrate were lysed with ACK lysis buffer. The cells (1×10^6/mL) were cultured in 24-well culture plates containing RPMI 1640 complete medium supplemented with GM-CSF (10

ng/mL), and the medium was changed every other days. After 7 days culture, loosely adherent and clustered cells were harvested and stimulated with LPS (1 μg/mL) for 24 h.

Renal subcapsular transplantation

LNSCs were transplanted in the renal subcapsular space of mice as described previously [26]. In brief, cultured LNSCs (2.5×10^5) were mixed with an equal number of LPS-stimulated BMDCs. The cell suspension was transferred to a sponge-like collagenous scaffold and immediately implanted in the renal subcapsular space of C57BL/6 mice. The grafts were harvested at 3 weeks after transplantation.

Reverse transcription and real-time PCR analysis

Total RNA extracted from cultured LNSCs, BMDCs, or renal subcapsular grafts with the use of Sepasol and an RNeasy Mini Kit was subjected to reverse transcription with the use of a QuantiTect Reverse Transcription Kit. The resulting cDNA was subjected to real-time PCR analysis in 384-well plates with the use of a QuantiTect SYBR Green PCR Kit and a LightCycler 480 instrument. The amplification results were analyzed with LightCycler 480 software, and the data were normalized by the amount of *Gapdh* mRNA. **Supporting Information Table 2** provides a list of primers.

Statistics

Quantitative data are presented as means ± SE and were analyzed by Student's *t* test, one-way ANOVA followed by Tukey's test, or two-way ANOVA followed by Sidak's test. A *P* value of <0.05 was considered statistically significant.

Acknowledgments

We thank Y. Takase, Y. Kanno, Y. Nakano, and D. Tanaka for technical assistance; and Y. Kobayashi and T. Watanabe (Kyoto University) for instruction on renal subcapsular transplantation. This work was supported by a Grant-in-Aid for Scientific Research (A) (to T.M.) and a Grant-in-Aid for Young Scientist (to Y.S.) from the Ministry of Education, Culture, Sports, Science, and Technology of Japan. S.K. was also supported by a scholarship provided by Nakatani Foundation.

Conflict of interest

The authors declare no commercial or financial conflict of interest.

References

1. **Malhotra, D.**, **Fletcher, A. L. and Turley, S. J.**, Stromal and hematopoietic cells in secondary lymphoid organs: partners in immunity. *Immunol. Rev*. 2013. **251**: 160–176.

2. **Mueller, S. N. and Germain, R. N.**, Stromal cell contributions to the homeostasis and functionality of the immune system. *Nat. Rev. Immunol*. 2009. **9**: 618–629.

3. **Alexandre, Y.O. and Mueller, S. N.**, Stromal cell networks coordinate immune response generation and maintenance. *Immunol. Rev*. 2018. **283**: 77–85.

4. **Fletcher, A. L.**, **Acton, S. E. and Knoblich, K.**, Lymph node fibroblastic reticular cells in health and disease. *Nat. Rev. Immunol*. 2015. **15**: 350–361.

5. **Bajénoff, M.**, **Koo, L. Y. and Germain, R. N.**, Stromal cell networks regulate lymphocyte entry, migration, and territoriality in lymph nodes. *Immunity* 2006. **25**: 989–1001.

6. **Cyster, J. G.**, Chemokines, sphingosine-1-phosphate, and cell migration in secondary lymphoid organs. *Annu. Rev. Immunol*. 2005. **23**: 127–159.

7. **Tewalt, E. F.**, **Cohen, J. N.**, **Rouhani, S. J. and Engelhard, V. H.**, Lymphatic endothelial cells - key players in regulation of tolerance and immunity. *Front. Immunol*. 2012. **3**: 305.

8. **Firner, S.**, **Onder, L.**, **Nindl, V. and Ludewig, B.**, Tight control - decision-making during T cell-vascular endothelial cell interaction. *Front. Immunol*. 2012. **3**: 279.

9. **Bar-Ephraim, Y. E. and Mebius, R. E.**, Innate lymphoid cells in secondary lymphoid organs. *Immunol. Rev*. 2016. **271**: 185–199.

10. **Roozendaal, R. and Mebius, R. E.**, Stromal cell-immune cell interactions. *Annu. Rev. Immunol*. 2011. **29**: 23–43.

11. **Corsiero, E.**, **Nerviani, A.**, **Bombardieri, M. and Pitzalis, C.** , Ectopic lymphoid structures: powerhouse of autoimmunity. *Front. Immunol*. 2016. **7**: 430.

12. **Acton, S. E.**, **Farrugia, A. J.**, **Astarita, J. L.**, **Mourão-Sá, D.**, **Jenkins, R. P.**, **Nye, E.**, **Hooper, S. et al.**, Dendritic cells control fibroblastic reticular network tension and lymph node expansion. *Nature* 2014. **514**: 498–502.

13. **Astarita, J. L.**, **Cremasco, V.**, **Fu, J.**, **Darnell, M. C.**, **Peck, J. R.**, **Nieves-Bonilla, J.M.**, **Song, K. et al.**, The CLEC-2-podoplanin axis controls the contractility of fibroblastic reticular cells and lymph node microarchitecture. *Nat. Immunol*. 2015. **16**: 75–84.

14. **Kumar, V.**, **Dasoveanu, D. C.**, **Chyou, S.**, **Tzeng, T-C.**, **Rozo, C.**, **Liang, Y.**, **Stohl, W. et al.**, A dendritic-cell-stromal axis maintains immune responses in lymph nodes. *Immunity* 2015. **42**: 719–730.

15. **Saito Y.**, **Respatika, D.**, **Komori, S.**, **Washio, K.**, **Nishimura, T.**, **Kotani, T.**, **Murata Y. et al.**, SIRPα^{+} dendritic cells regulate homeostasis of fibroblastic reticular cells via TNF receptor ligands in the adult spleen. *Proc. Natl. Acad. Sci. USA*. 2017. **114**: 201711345–E10160.

16. **Fletcher, A. L.**, **Malhotra, D.**, **Acton, S. E.**, **Lukacs-Kornek, V.**, **Bellemare-Pelletier, A.**, **Curry, M.**, **Armant, M. et al.**, Reproducible isolation of lymph node stromal cells reveals site-dependent differences in fibroblastic reticular cells. *Front. Immunol*. 2011. **2**: 35.

17. **Saito, Y.**, **Iwamura, H.**, **Kaneko, T.**, **Ohnishi, H.**, **Murata, Y.**, **Okazawa, H.**, **Kanazawa, Y. et al.**, Regulation by SIRPα of dendritic cell homeostasis in lymphoid tissues. *Blood* 2010. **116**: 3517–3525.

18. **Barclay, A. N. and van den Berg, T. K.**, The interaction between signal regulatory protein alpha (SIRPα) and CD47: structure, function, and therapeutic target. *Annu. Rev. Immunol*. 2014. **32**, 25–50.

19. **Murata, Y.**, **Kotani, T.**, **Ohnishi, H. and Matozaki, T.**, The CD47-SIRPα signalling system: its physiological roles and therapeutic application. *J Biochem*. 2014. **155**: 335–344.

20. **Fletcher, A. L.**, **Malhotra, D.**, **Acton, S. E.**, **Lukacs-Kornek, V.**, **Bellemare-Pelletier, A.**, **Curry, M.**, **Armant, M. et al.**, Reproducible isolation of lymph node stromal cells reveals site-dependent differences in fibroblastic reticular cells. *Front. Immunol*. 2011. **2**: 35.

21. **Sixt, M.**, **Kanazawa, N.**, **Selg, M.**, **Samson, T.**, **Roos, G.**, **Reinhardt, D. P.**, **Pabst, R. et al.**, The conduit system transports soluble antigens from the afferent lymph to resident dendritic cells in the T cell area of the lymph node. *Immunity* 2005. **22**: 19–29.

22. **Weih, F. and Caamano, J.**, Regulation of secondary lymphoid organ development by the nuclear factor-κB signal transduction pathway. *Immunol. Rev*. 2003. **195**: 91–105.

23. **Dejardin, E.**, **Droin, N. M.**, **Delhase, M.**, **Haas, E.**, **Cao, Y.**, **Makris, C.**, **Li, Z-W. et al.**, The lymphotoxin-β receptor induces different patterns of gene expression via two NF-κB pathways. *Immunity* 2002, **17**: 525–535.

24. **Lo, J.C.**, **Basak, S.**, **James, E. S.**, **Quiambo, R. S.**, **Kinsella, M.C.**, **Alegre, ML.**, **Weih, F. et al.**, Coordination between NF-κB family members p50 and p52 is essential for mediating LTβR signals in the development and organization of secondary lymphoid tissues. *Blood* 2006, **107**: 1048–1055.

25. **Tan, J. K. H. and Watanabe, T.**, Murine spleen tissue regeneration from neonatal spleen capsule requires lymphotoxin priming of stromal cells. *J. Immunol*. 2014. **193**: 1194–120.

26. **Suematsu, S. and Watanabe, T.**, Generation of a synthetic lymphoid tissue-like organoid in mice. *Nat. Biotechnol*. 2004. **22**: 1539–1545.

27. **Onder, L.**, **Narang, P.**, **Scandella, E.**, **Chai, Q.**, **Iolyeva, M.**, **Hoorweg, K.**, **Halin, C. et al.**, IL-7-producing stromal cells are critical for lymph node remodeling. *Blood* 2012. **120**: 4675–4683.

28. **Perez-Shibayama, C.**, **Gil-Cruz, C.**, **Cheng, H.W.**, **Onder, L.**, **Printz, A.**, **Mörbe, U.**, **Novkovic, M.**, **et al.**, Fibroblastic reticular cells initiate immune responses in visceral adipose tissues and secure peritoneal immunity. *Sci. Immunol.* 2018. **3**:eaar4539.

29. **Washio, K.**, **Kotani, T.**, **Saito, Y.**, **Respatika, D.**, **Murata, Y.**, **Kaneko, Y.**, **Okazawa, H.**, **et al.**, Dendritic cell SIRPα regulates homeostasis of dendritic cells in lymphoid organs. *Genes Cells* 2015. **20**:451–463.

30. **Cossarizza, A.**, **Chang, H.D.**, **Radbruch, A.**, **Akdis, M.**, **Andrä, I.**, **Annunziato, F.**, **Bacher, P.**, **et al.**, Guidelines for the use of flow cytometry and cell sorting in immunological studies. *Eur. J. Immunol.* 2017. **47**:1584–1797.

Figure Legends

Figure 1. Characterization of primary cultured LNSCs. (A) Generation of LNSCs from peripheral LNs. (B) Representative flow cytometry plots for FRCs, LECs, BECs, and DN cells among $CD45^-$ stromal cells on day 0 and day 6. SSC, side scatter. (C) The frequency of FRCs, LECs, BECs, and DN cells among $CD45^-$ stromal cells on day 6 determined as in (B). Data are means + SE for three independent experiments, each performed in triplicate with cells pooled from three mice. (D) Fluorescence microscopic analysis of F-actin as well as of Pdpn and Desmin (red). Nuclei were stained with DAPI (blue). Scale bar, 50 μm. (E) Staining for MHC I, MHC II or CD44 (open traces) or with an isotype control antibody (filled traces) on FRCs or LECs among $CD45^-$ stromal cells on day 6. (F) LNSCs (day 6) were incubated overnight and further cultured for 5 days in the presence of rTNF-α or a mAb to LTβR. Data are presented as fold increase in the number of $CD45^-$ cells relative to time 0, and they are means ± SD of triplicate determinations. (G) *Vcam1*, *Icam1*, *Ccl19, Ccl21,* and *Il7* mRNA abundance in LNSCs treated with the mAb to LTβR (5 μg/mL) for the indicated times. Data are expressed relative to the value for time 0, and are means + SE from three independent experiments, each performed in triplicate. ND, not detectable. Data in (B) and (D-F) are representative of three independent experiments. $*p < 0.05$, $**p < 0.01$, $***p < 0.001$ by one-way ANOVA and Tukey's test (C and G) or by two-way ANOVA and Sidak's test (F).

Figure 2. Importance of SIRPα on DCs for the proliferation of LNSCs. (A) LNSCs were cultured for the indicated times with LPS-stimulated BMDCs derived from control ($Sirpa^{f/f}$) or $Sirpa^{\Delta DC}$ mice, and the number of $CD45^-$ cells were determined. Data are means ± SE of triplicate determinations and are representative of two independent experiments. $***p < 0.001$ (two-way ANOVA and Sidak's test). (B) Relative mRNA abundance of *Tnf, Il6,* and *Il10* in BMDCs isolated from $Sirpa^{f/f}$ or $Sirpa^{\Delta DC}$ mice after

stimulation with LPS. Data are the means + SE of four mice per group from two independent experiments. * $p < 0.05$ (one-way ANOVA and Tukey's test)

Figure 3. DCs promote the development of LNSCs and recruitment of T cells in renal subcapsular transplants. (A) Schematic of renal subcapsular transplantation of LNSCs with LPS-stimulated BMDCs. (B) Immunofluorescence analysis of grafts containing LNSCs alone or LNSCs plus BMDCs for ER-TR7 and Thy1.2 staining. The boxed areas in the upper panels are shown at higher magnification in the lower panels. Scale bar, 100 μm. The ER-TR7$^+$ area in images was measured, and quantitative data are means + SE of four transplants per group from three independent experiments. (C) Total numbers of CD45$^+$ cells as well as of T cells, B cells, DCs, and granulocytes in LNSCs alone or LNSCs plus DCs grafts were shown. Data are means + SE of three transplants per group from two independent experiments. (D) The relative abundance of *Ccl19* mRNA in LNSCs alone or LNSCs plus DCs grafts. Data are means + SE for three transplants per group. (E) The grafts containing LNSCs with BMDCs from *Sirpa*$^{f/f}$ or *Sirpa*$^{\Delta DC}$ mice were stained for ER-TR7 and Thy1.2. Scale bar, 100 μm. The ER-TR7$^+$ area in images was measured, and quantitative data are means + SE of five transplants per group from two independent experiments. (F) Total numbers of CD45$^+$ cells, as well as of T cells, B cells, DCs, and granulocytes, in grafts were shown. Data are means + SE of seven transplants per group from three independent experiments. *$p < 0.05$, ***$p < 0.001$ (Student's *t* test).

Figure 1

S. Komori *et al.*

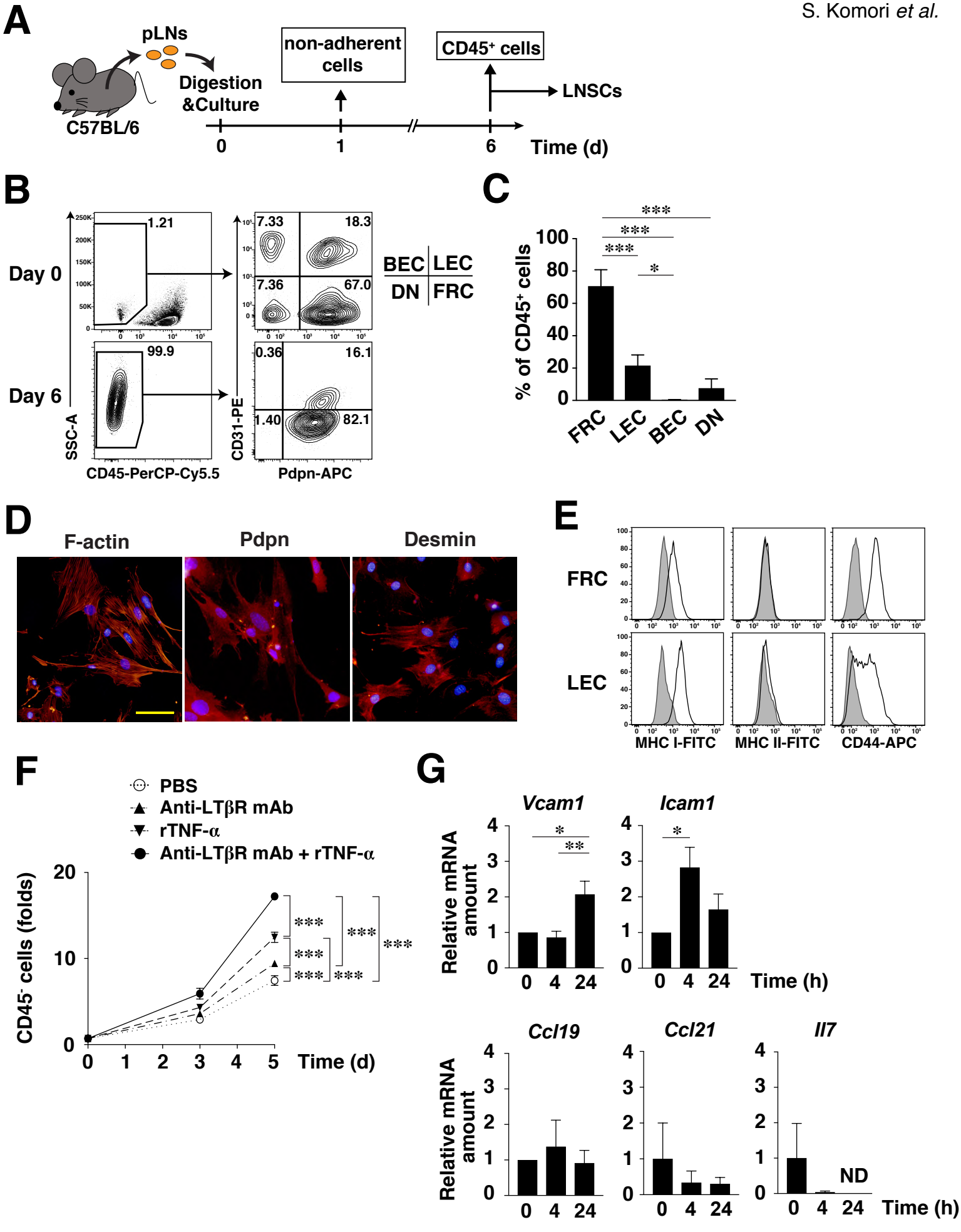

Figure 2

S. Komori *et al.*

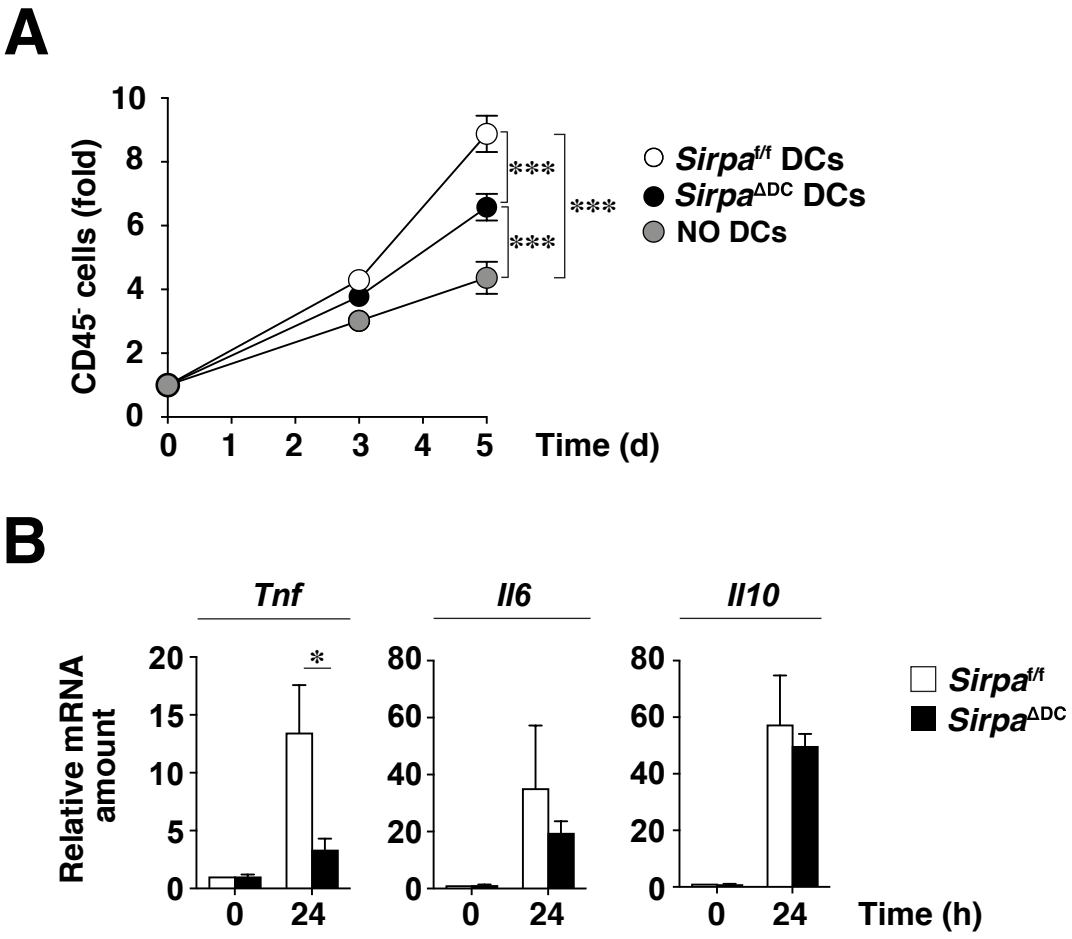

Figure 3

S. Komori *et al.*

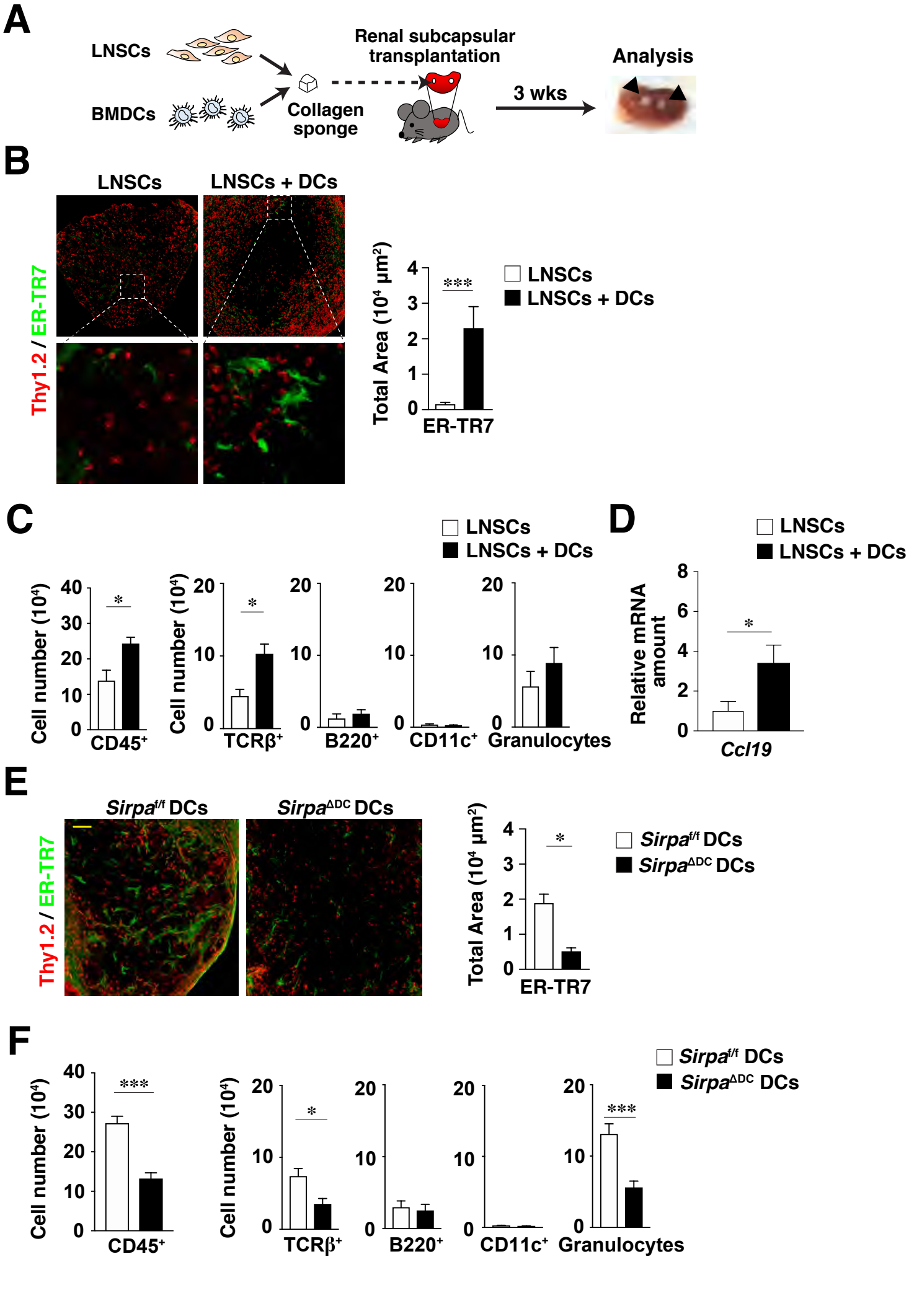

Supporting Information Fig. 1

S. Komori *et al.*

A

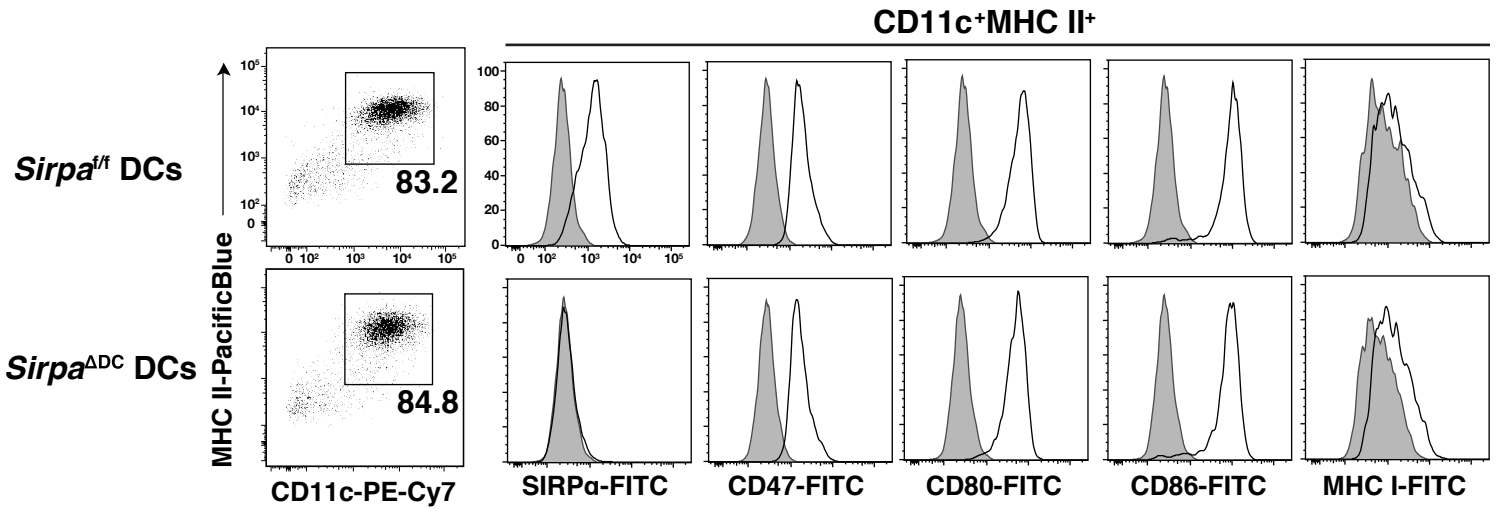

Supporting Information Fig. 1. Expression of surface marker on BMDCs. LPS-stimulated BMDCs from *Sirpa*$^{f/f}$ or *Sirpa*$^{\Delta DC}$ mice were stained for CD11c and MHC II, as well as for SIRPα, CD47, CD80, CD86 and MHC I (open traces), or with isotype control Abs (filled traces). The expression of SIRPα, CD47, CD80, CD86 and MHC I among CD11c^{+}MHCII^{+} cells were analyzed by flow cytometry. Data are representative of two independent experiments, each performed with two mice per group.

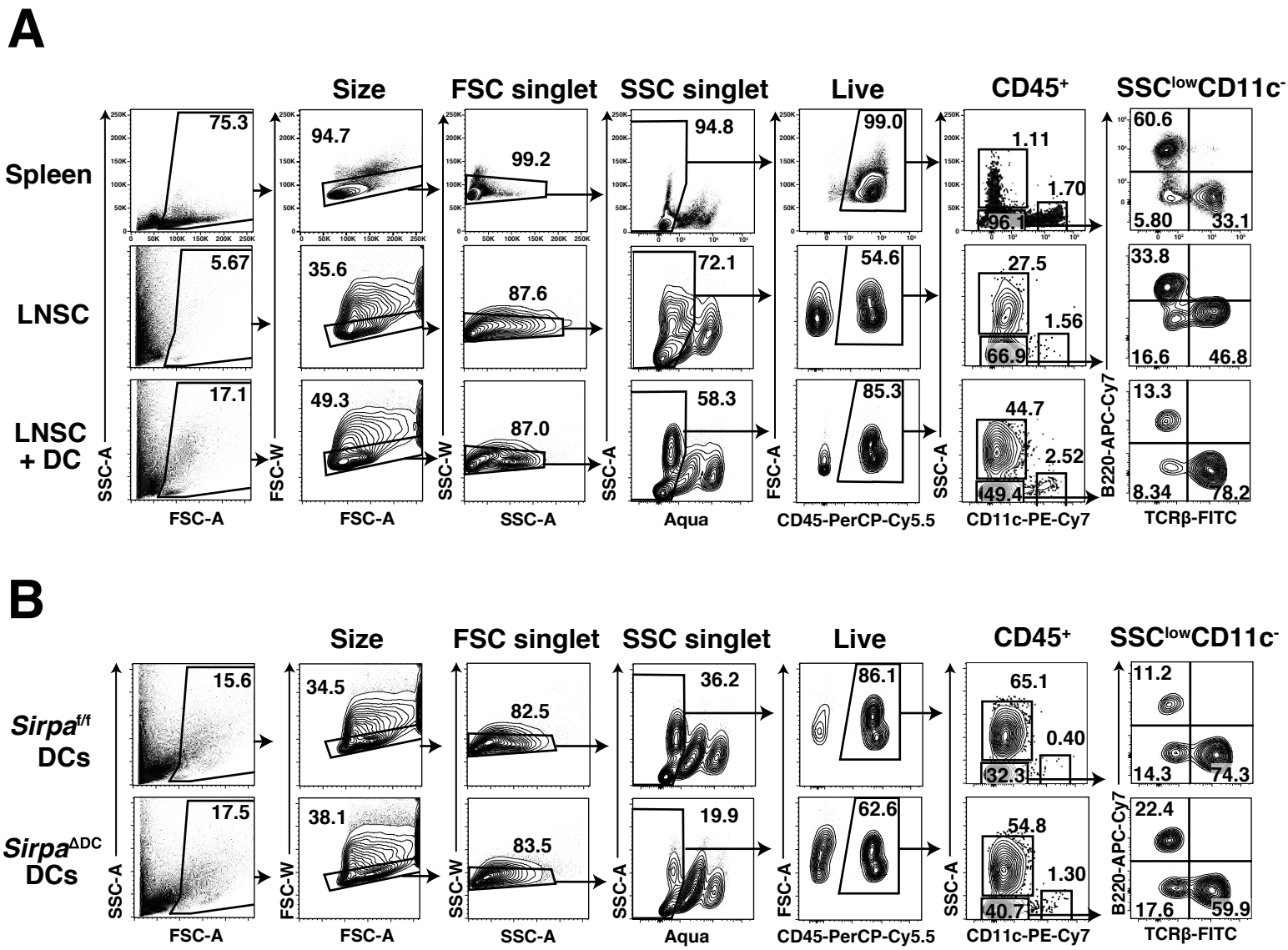

Supporting Information Fig. 2. Gating strategy for flow cytometric analysis of transplanted LNSCs. Representative flow cytometric plots showing the gating strategy and frequency of T cells, B cells, DCs, and granulocytes are presented for the C57BL/6 mouse spleen (control) as well as for transplanted LNSCs alone or LNSCs plus BMDCs (A) and for transplanted LNSCs plus BMDCs derived from *Sirpa*$^{f/f}$ or *Sirpa*$^{\Delta DC}$ mice (B). Cells were gated first based on forward scatter (FSC)–A and side scatter (SSC)–A intensity (first columns), after which FSC and SSC singlet cells (second and third columns) as well as Aqua$^-$ viable cells (fourth columns) were gated followed by CD45$^+$ cells (fifth columns). CD45$^+$ cells were then subdivided as SSC^{hi}CD11c$^-$ granulocytes, SSC^{lo}CD11c$^+$ DCs, and SSC^{lo}CD11c$^-$ cells (sixth columns). T cells and B cells were defined as TCRβ$^+$ B220$^-$ cells and TCRβ$^-$ B220$^+$ cells, respectively, among SSC^{lo}CD11c$^-$ cells (seventh columns).

Supporting Information Fig. 3

S. Komori *et al.*

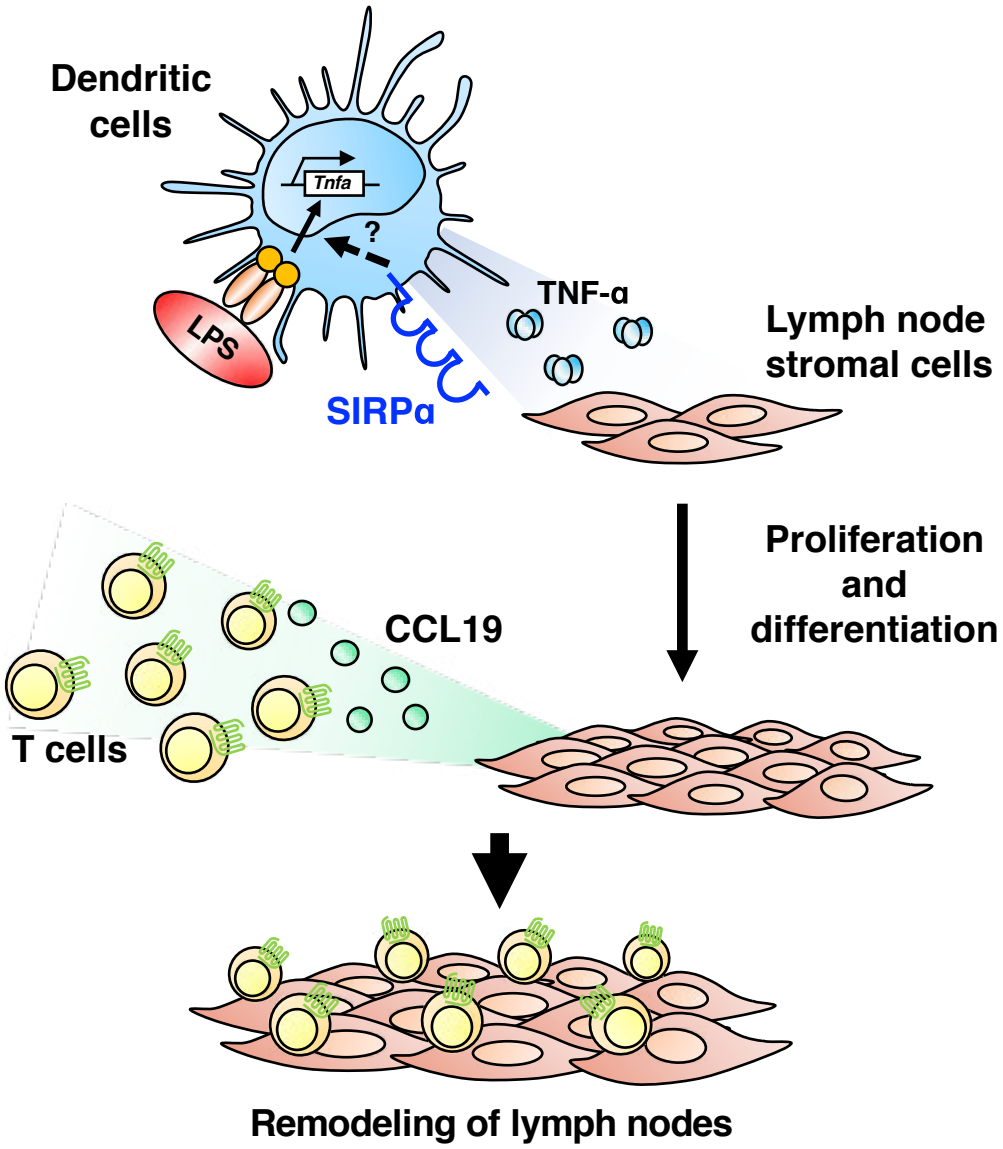

Supporting Information Fig. 3. Model for the role of SIRPα in the regulation of lymph node stromal cells (LNSCs) by dendritic cells (DCs). SIRPα$^+$ DCs control TNF-α production upon stimulation with LPS and promote LNSC proliferation *in vivo*. LNSCs in turn upregulate CCL19 production, which likely promotes the attraction of T cells and subsequently induces remodeling of lymph nodes.

Supporting Information Table 1

S. Komori *et al.*

Antibodies, reagents, and resources used in this study

REAGENT or RESOURCE	SOURCE	IDENTIFIER
Antibodies		
Purified anti-LTβR (clone 4H8)	Provided by C.F.Ware	N/A
Purified anti-ER-TR7 (clone ER-TR7)	BMA Biomedicals	CAT#T-2109
Purified anti-Pdpn (clone eBio8.1.1)	eBioscience	CAT#14-5381-82
Purified anti-desmin (clone Y-20)	Santa Cruz Biotechnology	CAT#sc-7559
Purified anti-CD16/32 (clone 93)	Biolegend	CAT#101302
FITC conjugated streptavidin	Biolegend	CAT#405202
FITC conjugated anti-Podoplanin (clone 8.1.1)	Biolegend	CAT#127415
FITC conjugated anti-MHC I (clone AF-88.5)	Biolegend	CAT#116505
PE conjugated anti-CD31 (clone MEC13.3)	Biolegend	CAT#102507
PerCP-Cy5.5 conjugated anti-CD45 (clone 30-F11)	Biolegend	CAT#103131
PE-Cy7 conjugated anti-CD11c (clone N418)	Biolegend	CAT#117318
APC conjugated anti-Podoplanin (clone 8.1.1)	Biolegend	CAT#127410
APC conjugated anti-CD44 (clone IM7)	Biolegend	CAT#103011
APC-Cy7 conjugated anti-B220 (clone RA3-6B2)	Biolegend	CAT#103224
Pacific Blue conjugated anti-MHC II (clone M5/114.15.2)	Biolegend	CAT#107620
Biotin conjugated anti-Thy1.2 (clone 30-H12)	eBioscience	CAT#13-0903-82
Biotin conjugated anti-TCRβ (clone H57-597)	Biolegend	CAT#109203
Biotin conjugated anti-MHC II (clone M5/114.15.2)	eBioscience	CAT#13-5321-81
Biotin conjugated anti-SIRPα (clone P84)	eBioscience	CAT#13-1721-82
Biotin conjugated anti-CD47 (clone miap301)	Biolegend	CAT#127505
Biotin conjugated anti-CD80 (clone 16-10A1)	eBioscience	CAT#13-0801-81
Biotin conjugated anti-CD86 (clone GL1)	eBioscience	CAT#13-0862-81
Zombie Aqua Fixable Viability Kit	Biolegend	CAT#423101
DAPI	Nacalai Tesque	CAT#11034-56
Rhodamine conjugated phalloidin	Thermo Fischer Scientific	CAT#R415
Alexa Fluor 488 conjugated goat anti-rat IgG	Invitrogen	CAT#A11006
Cy3 conjugated donkey anti-hamster IgG	Jackson ImmunoResearch Laboratories	CAT#127-165-160
Cy3 conjugated streptavidin	Jackson ImmunoResearch Laboratories	CAT#016-160-084
Chemicals, Peptides, and Recombinant Proteins		
Recombinant Mouse TNF-α	Peprotech	CAT#315-01A
Recombinant Mouse GM-CSF	Peprotech	CAT#315-03
Lipopolysaccharide (LPS)	Sigma-Aldrich	CAT#L3012
Collagenase P	Roche	CAT#11213857001
Dispase II	Roche	CAT#04942078001
Deoxyribonuclease I (DNase I)	Worthington	CAT#LS002139
Critical Commercial assay		
CD45 magnetic beads	Miltenyi Biotec	CAT#130-052-301
RNeasy Mini Kit	Qiagen	CAT#74104
Sepasol	Nacalai Tesque	CAT#09379-55
QuantiTect Reverse Transcription Kit	Qiagen	CAT#205313
QuantiTect SYBR Green PCR Kit	Qiagen	CAT#204143
Collagen sponge	KOKEN	CAT#CS-35
Tissue-Tec O.C.T	Sakura Finetechnical	CAT#4557
Experimental Models: Organisms / Strains		
Mouse: C57BL/6J	Japan SLC	N/A
Mouse: CD11c-*Cre*	Jackson Laboratories	CAT#008068
Mouse: *Sirpa*^{tf}	Washio et al., 2015	N/A
Mouse: CD11c-*Cre;Sirpa*^{tf}	Washio et al., 2015	N/A
Softwares		
FlowJo v10	FlowJo, LLC	https://www.flowjo.com/solutions/flowjo
ImageJ	National Institutes of Health	http://www.imagej.nih.gov/ij
Prism 7.0c	GraphPad Software Inc.	https://www.graphpad.com
Adobe Photoshop	Adobe Inc.	https://www.adobe.com
Other		
autoMACS Pro Separator	Miltenyi Biotec	N/A
BD FACSVerse	BD Biosciences	N/A
BZ-X700	Keyence	N/A
LightCycler 480 instrument	Roche	N/A

Supporting Information Table 2

S. Komori *et al.*

Primers used for QPCR analysis

Gene	Forward primer sequence	Reverse primer sequence
Gapdh	5'- AGGTCGGTGTGAACGGATTTG -3'	5'- TGTAGACCATGTAGTTGAGGTCA -3'
Vcam1	5'- CCGGCATATACGAGTGTGAAT -3'	5'- ATGGCAGGTATTACCAAGGAAGAT -3'
Icam1	5'- GTTTAAAAACCAGACCCTGGAACT -3'	5'- CGTCTGCAGGTCATCTTAGGAG -3'
Ccl19	5'- GGGGTGCTAATGATGCGGAA -3'	5'- CCTTAGTGTGGTGAACACAACA -3'
Ccl21	5'- ATCCCGGCAATCCTGTTCTC -3'	5'- GGGGCTTTGTTTCCCTGGG -3'
Il7	5'- GATAGTAATTGCCCGAATAATGAACCA -3'	5'- GTTTGTGTGCCTTGTGATACTGTTAG -3'
Tnf	5'- TGGAACTGGCAGAAGAGGCACT -3'	5'- GAGATAGCAAATCGGCTGACGG -3'
Il6	5'- TAGTCCTTCCTACCCCAATTTCC -3'	5'- TTGGTCCTTAGCCACTCCTTC -3'
Il10	5'- GCTCTTACTGACTGGCATGAG -3'	5'- CGCAGCTCTAGGAGCATGTG -3'